JOURNAL OF SOLID STATE CHEMISTRY 39, 128–132 (1981)

Coordination and Bonding in Fe_3P–Ti_3P–V_3S–Ta_3As-Type Compounds: The Crystal Structures of Hf_3Sb and *h*-Ta_3Ge

JAN-OLOV WILLERSTRÖM AND STIG RUNDQVIST

Institute of Chemistry, University of Uppsala, Box 531,
S-751 21 Uppsala, Sweden

Received January 29, 1981

Interatomic distances in Hf_3Sb and *h*-Ta_3Ge (Fe_3P-type structure, space group $I\bar{4}$, $Z = 8$) have been determined by crystal structure refinements based on Rietveld-type full-profile analyses of Guinier–Hägg X-ray powder film intensity data. The results, together with data from the recently refined Hf_3As and Ta_3As structures, are included in a survey of coordination and bonding in Fe_3P–Ti_3P–V_3S–Ta_3As-type compounds. It is shown that the trends in atomic coordination observed can be explained in terms of an interplay of *d–d* and *d–p* electronic interactions.

Introduction

Coordination and bonding in compounds crystallizing with the closely related structure types Fe_3P, Ti_3P, α-V_3S and β-V_3S were discussed in a recent article (*1*). The conclusions were mainly based on results for phosphides, since structural information on compounds containing nonmetals other than phosphorus was very limited. In order to obtain material for further analysis we have carried out refinements of the structures of Hf_3Sb and *h*-Ta_3Ge. The results reported here provide the first structure data for antimonide and germanide representatives of the structure family mentioned above.

Hf_3Sb and *h*-Ta_3Ge both crystallize with the Fe_3P-type structure (*2*), space group $I4$ (No. 82), $Z = 8$. *h*-Ta_3Ge is a high-temperature form of Ta_3Ge, the low-temperature form *l*-Ta_3Ge crystallizing with the Ti_3P-type structure (*2*).

The *h*-Ta_3Ge/*l*-Ta_3Ge transformation is presently being studied in detail; the results will be reported elsewhere (*3*).

Experimental Details

The compounds were prepared by arc-melting mixtures of the constituent elements under a purified argon atmosphere. To compensate for losses due to evaporation, antimony and germanium were added in slight excess over the ideal stoichiometric formula. The following starting materials were used: Hafnium containing 3% zirconium, claimed purity 3N disregarding zirconium (Koch–Light); antimony, claimed purity 6N (Johnson, Matthey & Co); tantalum, claimed purity 3N5 (Koch–Light); and zone-refined germanium.

The products were examined by X-ray powder diffraction, using a Philips XDC 700 Guinier–Hägg-type focusing camera with $CuK\alpha_1$ radiation and germanium, $a = 5.657906$ Å (*4*), or a mixture of germanium and silicon, $a = 5.431065$ Å (*5*), as internal

0022-4596/81/100128-05$02.00/0

calibration standards. Unit cell dimensions were refined by the least-squares method using the local program CELNE (*6*).

Structure refinements were performed by the least-squares method using a Rietveld-type full-profile analysis of the Guinier–Hägg powder film intensity data (*7*). The intensity data were obtained using a SAAB automatic film scanner (*8*, *9*) connected to an IBM 1800 computer.

The Hf_3Sb sample was single-phase, while the *h*-Ta_3Ge sample contained minor amounts of tantalum metal. The tantalum reflections were removed from the profile data without any loss of intensity information for *h*-Ta_3Ge.

Structure Refinements

The following parameters were refined for each compound: *profile parameters*—halfwidth (*3*), asymmetry (*1*), 2θ-zero-point (*1*); *structure parameters*—overall scale factor (*1*), lattice parameters (*2*), positional parameters (*12*), isotropic temperature factors (*2*). Scattering factors, corrected for the anomalous dispersion, were interpolated from values given in the "International Tables" (*10*). No attempts were made to correct for absorption. The temperature factor values (one common for the metal atoms and one for the nonmetal atoms) are therefore an unknown combination of thermal vibration and absorption effects.

Positional parameters derived from the Ta_3Si (*2*) structure were used as starting values in the refinement of *h*-Ta_3Ge, while the starting values for Hf_3Sb were derived from the Hf_3As structure (*11*). The final residual values obtained (for definitions see Malmros and Thomas (*7*)) were for Hf_3Sb (147 reflections): $R_I = 0.079$, $R_F = 0.062$, $R_p = 0.156$, $R_{wp} = 0.202$, and for *h*-Ta_3Ge (121 reflections): $R_I = 0.080$, $R_F = 0.055$, $R_p = 0.159$ and $R_{wp} = 0.206$.

Structure data are presented in Table I, and interatomic distances in Table II.

Discussion of the Results

In an earlier study (*1*), the atomic coordination in various representatives of the Fe_3P–Ti_3P–V_3S structure family was examined. The most conspicuous feature revealed by the examination was associated with the transition metal atom environment about the nonmetal atoms. The number of near metal atom neighbours was found to vary from eight to nine in a way which was neither consistent with size factor effects nor with simple valency or electron concentration rules. In order to explain the coordination trends observed, a qualitative model for the chemical bonding in the M_3X (M = transition metal, X = nonmetal) family of compounds was proposed as follows.

The *d* electrons of the M atoms form a metallic band similar to that in the elemental M component. The valency electrons of the X atoms interact with the *d* band to form a covalent type of M–X bonding involving electronic states formed by an admixture of nonmetal *p* and transition metal *d* orbitals. The bonding situation in the M_3X

TABLE I

STRUCTURE DATA FOR Hf_3Sb AND *h*-Ta_3Ge^a

Atom	*x*	*y*	*z*	*B* (Å²)
Hf(1)	0830(5)	1082(5)	2081(8)	1.24(6)
Hf(2)	3544(4)	0238(5)	9818(11)	
Hf(3)	1880(5)	2143(5)	7641(9)	
Sb	2902(6)	0333(6)	4805(14)	1.5(1)
Ta(1)	0834(5)	1002(5)	2335(11)	1.50(6)
Ta(2)	3562(4)	0180(6)	9891(13)	
Ta(3)	1928(5)	2128(5)	7561(11)	
Ge	2942(9)	0261(10)	4703(27)	0.9(2)

[a] Space group $I\bar{4}$ (No. 82); all atoms in position 8*g*; Hf_3Sb: $a = 11.1899(3)$ Å, $c = 5.6364(2)$ Å; *h*-Ta_3Ge: $a = 10.3421(3)$ Å, $c = 5.1532(2)$ Å. Positional parameters × 10^4, standard deviations in parentheses.

TABLE II

INTERATOMIC DISTANCES IN Hf_3Sb AND h-Ta_3Ge[a]

Hf(1)–	Sb	2.905(9)	Ta(1)–	Ge	2.613(12)
	Sb	2.988(9)		Ta(1)	2.696(10)
	Hf(3)	3.008(7)		Ge	2.764(13)
	Hf(1)	3.054(11)		Ta(3)	2.948(8)
	Hf(2)	3.188(7)		Ta(3)	3.019(7)
	2Hf(1)	3.188(9)		Ta(2)	3.070(7)
	Hf(3)	3.256(8)		2Ta(1)	3.070(10)
	Hf(2)	3.426(7)		Ta(3)	3.145(8)
	Hf(3)	3.448(7)		Ta(2)	3.204(7)
	Hf(3)	3.551(7)		Ta(3)	3.210(8)
	Hf(3)	3.630(8)		Ta(3)	3.313(7)
	2Hf(1)	3.937(9)		2Ta(1)	3.343(10)
Hf(2)–	Sb	2.895(8)	Ta(2)–	Ge	2.562(15)
	Sb	2.903(10)		Ge	2.624(11)
	Sb	2.908(8)		Ge	2.627(11)
	Sb	2.917(10)		Ge	2.751(15)
	Hf(3)	3.085(7)		Ta(3)	2.890(8)
	Hf(3)	3.183(7)		Ta(3)	2.946(8)
	Hf(2)	3.302(9)		Ta(2)	2.998(9)
	Hf(3)	3.368(7)		Ta(3)	3.147(8)
	2Hf(2)	3.505(10)		2Ta(2)	3.250(11)
	2Hf(2)	3.820(10)		2Ta(2)	3.425(11)
				Ta(3)	3.662(8)
Hf(3)–	Sb	2.822(9)			
	Sb	2.959(8)	Ta(3)–	Ge	2.646(13)
	Sb	3.086(8)		Ge	2.682(12)
	2Hf(3)	3.241(5)		Ge	2.921(12)
				2Ta(3)	2.938(5)
				Ge	3.724(12)

[a] Distances shorter than 4 Å are listed, estimated standard deviations in parentheses.

compounds can accordingly be regarded as an interplay between d–d and d–p interactions. Changes in this interplay might affect the atomic coordination. For instance, if the d states corresponding to the M–M bonding are progressively filled, a smaller fraction of the d states would presumably become available for bonding d–p interactions, leading to a decreasing metal atom coordination about the nonmetal atoms. This hypothesis would explain an empirical rule found for the phosphide representatives, viz.: "the greater the cohesive strength of the parent transitional metal, the smaller is the phosphorus coordination number in the corresponding phosphide" (*1*). The d–d bonding interactions, which are mainly responsible for the cohesive properties of the pure transition metals, were assumed to follow the same trend in the M_3P phosphides as in the corresponding M components.

The discussion of coordination and bonding in the Fe_3P–Ti_3P–V_3S family of compounds was initially restricted to the phosphide representatives, since the structural information on compounds with p elements other than phosphorus was rather meagre. With the present results, data are now available for a germanide and an antimonide, and recent structure determinations have provided data also for Hf_3As (*11*) and Ta_3As (*12*). These two compounds are isostructural and crystallize with a monoclinic symmetry, while the Fe_3P–Ti_3P–V_3S-type compounds all have tetragonal symmetries. The atomic arrangements in Hf_3As and Ta_3As are so similar to those in the tetragonal M_3X compounds, however, that the family relationship is evident (*11*). The two arsenides are therefore included in the present discussion.

The nonmetal atom coordination in Hf_3Sb, h-Ta_3Ge, Hf_3As, Ta_3As, and a selected number of further family representatives is illustrated histographically in Fig. 1. The histograms indicate the number of M–X distances falling within given intervals of D/d, where D is a scale factor equal to the sum of the Goldschmidt radius for 12-coordination for the metal atom and the covalent radius for the nonmetal atom, and d is the M–X interatomic distance. For further details of the histographic representation, see (*1*). The following observations can be made from Fig. 1.

In the case of the arsenides, the ninth metal atom neighbor is more distant from the central arsenic atoms in Ta_3As than in Hf_3As. This would be expected if the empirical rule for phosphides as mentioned above is also valid for arsenides. On the

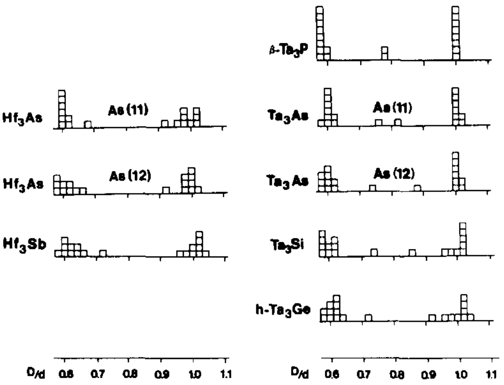

FIG. 1. Histographic representation of the coordination of metal (*M*) atoms about the nonmetal (*X*) atoms in some representatives of the Fe_3P–Ti_3P–V_3S–Ta_3As structure family. Each square corresponds to one interatomic distance. *D* is the sum of the Goldschmidt radius for the metal atom and the covalent radius for the nonmetal atom, and *d* is the *M*–*X* interatomic distance.

other hand, the opposite coordination trend would be predicted from size-factor considerations.

The nonmetal atom coordination is rather similar for Hf_3As and Hf_3Sb, the tendency to form an even nine-coordination being more pronounced for Sb.

For the tantalum compounds, there is an increasing tendency toward an eight-coordination for the nonmetal atoms in the series Ta_3Ge, Ta_3Si, Ta_3As, Ta_3P. An analogous observation can be made for the niobium representatives (*1*). Sulfur tends to have a lower coordination than phosphorus, as shown by a comparison between V_3P and α-V_3S or β-V_3S (*1*).

If the coordination trends observed are assumed to reflect changes in the magnitude of the *d*–*p* interaction, this interaction would accordingly increase in the sequence S, P, As, Si, Ge, Sb. (The position of Sb is somewhat uncertain but a structure refinement of Hf_3Ge might clarify the situation.) This order would be retained if the elements were arranged with decreasing electronegativity (Phillips' electronegativity scale (*13*)), while the order of Si and As would be reversed if they were arranged according to increasing covalent radii.

It is interesting to observe that band structure calculations made for the monoxides, mononitrides, and monocarbides of transition metals from groups III to V in the periodic table clearly indicate an increasing degree of *d*–*p* mixing on passing from oxides to nitrides to carbides, that is: with decreasing nonmetal electronegativity (*14*). Band structure calculations have not been made for any compound of the Fe_3P–Ti_3P–V_3S–Ta_3As family so far.

Following the present line of reasoning it is possible to make some simple predictions for those structure family members for which no detailed crystallographic information is yet available. A fairly even nine-coordination for the nonmetal atoms should obtain in Y_3Sb, Ti_3Si, Ti_3Ge, Ti_3As, Zr_3Si, Zr_3Ge, Zr_3As and Zr_3Sb, while a pronounced tendency towards eight-coordination should be evident in Hf_3P and *l*-Ta_3Ge, and less so in Hf_3Ge.

In conclusion, the hypothesis of a *d*–*d*/*d*–*p* electronic interplay appears to provide a fruitful approach to a better understanding of the crystal chemistry of transition metal compounds with nonmetals having unfilled *p* levels. As indicated by the present study, the coordination trends observed in the large family of Fe_3P–Ti_3P–V_3S–Ta_3As-type compounds can be rationalized in terms of this hypothesis.

Acknowledgment

Financial support from the Swedish Natural Science Research Council is gratefully acknowledged.

References

1. S. RUNDQVIST, Y. ANDERSSON, AND S. PRAMATUS, *J. Solid State Chem.* **28**, 41 (1979).

2. W. ROSSTEUTSCHER AND K. SCHUBERT, *Z. Metallk.* **56**, 813 (1965).

3. J.-O. WILLERSTRÖM, to be published.

4. J. F. C. Baker and M. Hart, *Acta Crystallogr. Sect. A* **31,** 364 (1975).
5. R. D. Deslattes and A. Henins, *Phys. Rev. Lett.* **31,** 972 (1973).
6. N. O. Ersson, Institute of Chemistry, Uppsala, unpublished.
7. G. Malmros and J. O. Thomas, *J. Appl. Crystallogr.* **10,** 7 (1977).
8. S. Abrahamsson, *J. Sci. Instrum.* **43,** 931 (1966).
9. "SAAB Film Scanner Manual," SAAB AB, Datasaab, Linköping, Sweden (1967).
10. "International Tables for X-Ray Crystallography," Vol. IV. Kynoch Press, Birmingham (1974).
11. J.-O. Willerström, B. Carlsson, and S. Rundqvist, *J. Solid State Chem.* **31,** 227 (1980).
12. Yu Wang, L. D. Calvert, E. J. Gabe, and J. B. Taylor, *Acta Crystallogr. Sect. B* **35,** 1447 (1979).
13. J. C. Phillips, *Rev. Mod. Phys.* **42,** 317 (1970).
14. A. Neckel, K. Schwarz, R. Eibler, P. Weinberger, and P. Rastl, *Ber. Bunsenges. Phys. Chem.* **79,** 1053 (1975).